EARTH SURFACE PROCESSES AND LANDFORMS
Earth Surf. Process. Landforms **46**, 307–319 (2021)

Published online 16 November 2020 in Wiley Online Library
(wileyonlinelibrary.com) DOI: 10.1002/esp.5025

Impact of an 0.2 km³ Rock Avalanche on Lake Eibsee (Bavarian Alps, Germany) – Part II: Catchment Response to Consecutive Debris Avalanche and Debris Flow

Sibylle Knapp,[1]* Flavio S. Anselmetti,[2] Bernhard Lempe[3] and Michael Krautblatter[1]
[1] Landslides Research Group, Technical University of Munich, Munich, Germany
[2] Institute of Geological Sciences and Oeschger Centre for Climate Change Research, University of Bern, Bern, Switzerland
[3] Engineering Geology, Technical University of Munich, Munich, Germany

Received 25 March 2020; Revised 1 October 2020; Accepted 3 October 2020

*Correspondence to: Sibylle Knapp, Landslides Research Group, Technical University of Munich, Munich, Germany. E-mail: sibylle.knapp@tum.de

ESPL
Earth Surface Processes and Landforms

ABSTRACT: The ~0.2 km³ Eibsee rock avalanche impacted Paleolake Eibsee and completely displaced its waters. This study analyses the lake impact and the consequences, and the catchment response to the landslide. A quasi-3D seismic reflection survey, four sediment cores from modern Lake Eibsee, reaching far down into the rock avalanche mass, nine radiocarbon ages, and geomorphic analysis allow us to distinguish the main rock avalanche event from a secondary debris avalanche and debris flow. The highly fluidized debris avalanche formed a megaturbidite and multiple swashes that are recorded in the lake sediments. The new calibrated age for the Eibsee rock avalanche of ~4080–3970 cal yr BP indicates a coincidence with rockslides in the Fernpass cluster and subaquatic landslides in Lake Piburg and Lake Plansee, and raises the possibility that a large regional earthquake triggered these events. We document a complex history of erosion and sedimentation in Lake Eibsee, and demonstrate how the catchment response and rebirth of the lake are revealed through the complementary application of geophysics, sedimentology, radiocarbon dating, and geomorphology. © 2020 The Authors. Earth Surface Processes and Landforms published by John Wiley & Sons Ltd.

KEYWORDS: rock avalanche; lake impact; lake sediments; catchment response; progressive slope failure; recurrence rates; prehistoric earthquake; Fernpass rockslide cluster

Introduction

Massive rock-slope failures often occur progressively in multiple stages from the same scarps or nearby scarps. Recent examples show that after an initial massive failure, a mountain flank may collapse again after a few days (e.g. Randa, Switzerland, 1991; Eberhardt *et al.*, 2004), a few years (e.g. Tangjiawan, China, 2008 and 2016; Fan *et al.*, 2018), or tens to hundreds of years (e.g. Mount Spitzstein, Switzerland, active again after events at ~2550, ~2250, ~2180, ~1720, and ~1320 cal yr BP; Knapp *et al.*, 2018). Yet, it is not possible to predict when and how often a scarp might be reactivated, and it is unclear what role the trigger and predisposing factors play in the catchment response. Clearly, however, refining recurrence rates and magnitudes is essential for future hazard assessment, and improving our understanding of progressive failure and catchment response after such catastrophic events.

The so-called 'Fernpass rockslide cluster' is a group of large rock-slope failures in the Northern Calcareous Alps and Central Eastern Alps (Figure 1a; Prager *et al.*, 2008). Many of these landslides occurred at or after the end of the Holocene climate optimum during the Subboreal (~4800–3800 cal yr BP; Wanner *et al.*, 2008, 2011). Researchers have made a lot of effort to bracket the ages of these landslides with different dating techniques to refine recurrence rates. Well-known examples are the rockslides at Fernpass (~4200–4100 cal yr BP; Prager *et al.*, 2009) and Tschirgant (~3010 cal yr BP; Ostermann *et al.*, 2017). However, all dating techniques carry uncertainties, and dating is sometimes too imprecise to recognize separate events, even though the deposit morphology suggests multistage failure (e.g. the Pletzachkogel and Köfels rockslides; Ivy-Ochs *et al.*, 1998; Hermanns *et al.*, 2006; Prager *et al.*, 2008; Patzelt, 2012b). Consequently, a new complementary approach is required to decipher the multistage character of ancient events.

The Eibsee rock avalanche, sourced at Mount Zugspitze in the Bavarian Alps, is part of the Fernpass rockslide cluster and has until now been considered a single failure dated at ~3700 yr BP (Jerz and Poschinger, 1995). In this paper, we present the results of geophysical and sedimentological investigations of Lake Eibsee, new radiocarbon ages from event deposits in the lake, and geomorphic observations. The data not only

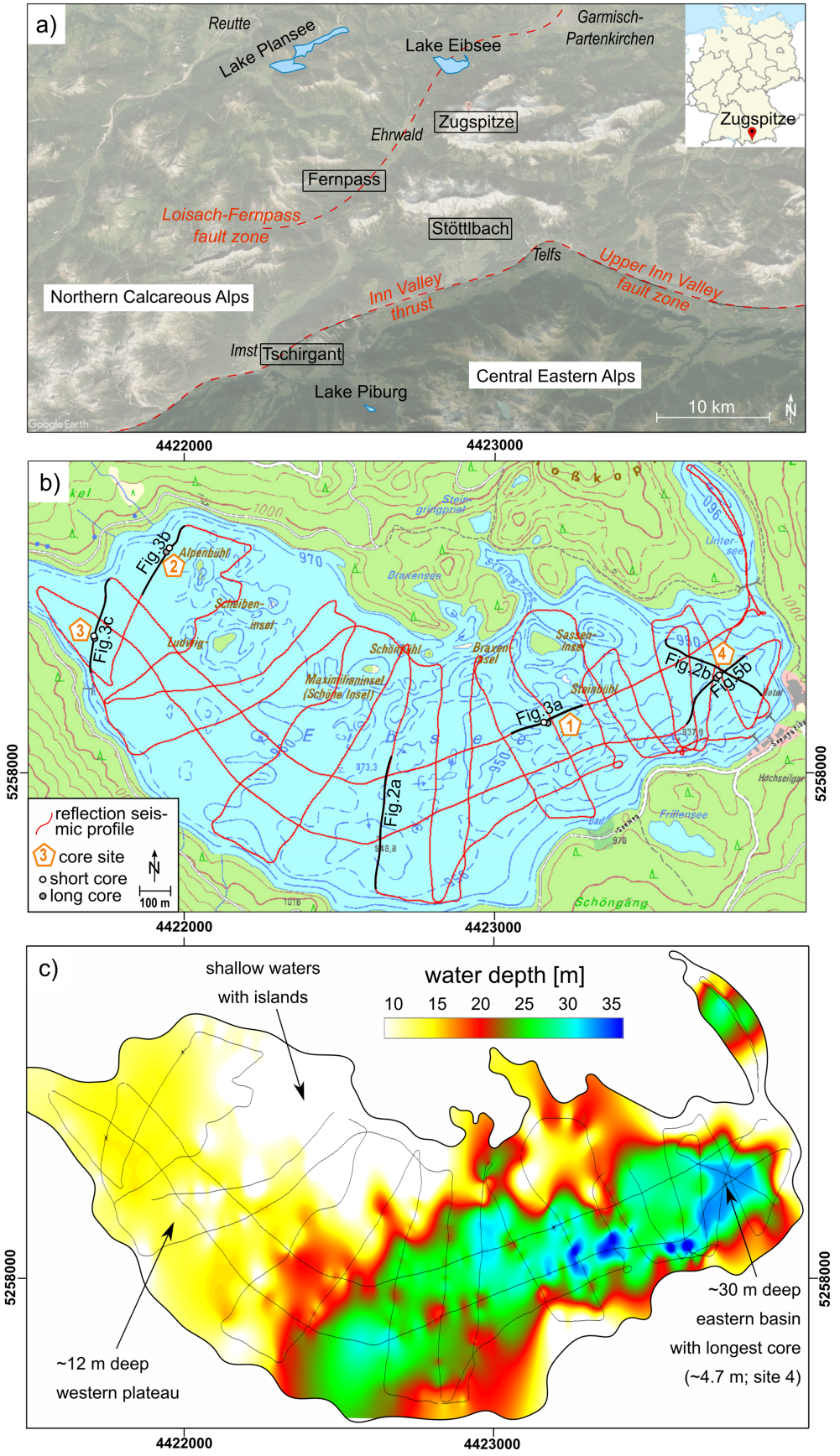

Figure 1. (a) Map of the region including Mount Zugspitze and Lake Eibsee in the Northern Calcareous Alps; landslides and fault zones related to the 'Fernpass cluster' are shown. Image © 2020 Maxar Technologies/Google Earth. (b) Map of Lake Eibsee and surroundings showing seismic reflection survey lines and core locations. Source of topographic map: Bavarian Surveying and Mapping Authority (2006). (c) Bathymetry of Lake Eibsee, interpolated from seismic data. Coordinates are given in Gauss-Krüger Zone 4. [Colour figure can be viewed at wileyonlinelibrary.com]

document three rock-slope failure events that we presume are related to each other, but also help to improve our understanding of how and under which circumstances a fragmenting rock mass may transform into or trigger a highly mobile debris avalanche or debris flow. The importance of this learning is highlighted by the massive rock-slope failure at Piz Cengalo in 2017 (Walter *et al.*, 2020), where secondary debris flows reached and destroyed settlements and other infrastructure, causing fatalities far beyond the reach of the original rock avalanche.

Our study addresses five research questions: Is the Eibsee rock avalanche a single failure, or can we decipher multistage events? What happens during and after the impact of the rock avalanche on the lake? Does a new lake form, and if so, how and where? Can we find evidence of a displaced paleolake in the modern lake? And, finally, what can we learn about progressive scarp evolution and repeated rock-slope failures that feature consecutive rock avalanche and debris flow events?

Study Site

Lake Eibsee (973 m a.s.l.) is located at the foot of Mount Zugspitze (2962 m a.s.l.), the highest summit in Germany, in the Loisach-Fernpass fault zone (Figure 1a). The lake has a surface area of ~1.8 km^2 and a maximum depth of ~36 m. It is mostly fed by groundwater; there are small surface water inflows from the west (Kotbach and Markgraben), and there is no outflowing stream. The lake shoreline is undulatory, and there are several small islands (Figure 1b), mainly in the western and middle parts of the lake, that consist of rock avalanche material (Wetterstein Limestone and some limestones and marlstones of the Alpine Muschelkalk, mostly Reifling Formation). Plattenkalk Limestone and Hauptdolomite bedrock are exposed north of the lake. A Paleolake Eibsee, larger than the modern one, existed at this site until the Eibsee rock avalanche impacted and destroyed it (see Part I, the companion to this article, Knapp *et al.*, 2020).

Methods

Seismic-reflection survey

Seismic surveys were carried out on Lake Eibsee in May 2015. The surveys were performed with an Octopus 760™ Geophysical Acquisition System with a single-channel 3.5 kHz pinger source/receiver. We operated the system with an inflatable boat travelling at a mean speed of 5–6 km h^{-1} to acquire a dense, quasi-three-dimensional grid of seismic profiles in the lake (Figure 1b). The seismic profiles were analysed with the KingdomSuite™ interpretation software. The conversion of two-way travel time to depth assumes a *P*-wave velocity of 1500 m s^{-1} for both water and lake sediments.

Lake-sediment coring

We cored lake sediments from a platform with an UWITEC percussion piston-coring system in October 2016. Long cores were recovered in 3 m-long, 63 mm-diameter PVC tubes. The cores were cut into three 1 m-long sections immediately after core recovery (e.g. core EIB16-02 was cut into three 1 m pieces EIB16-02A, -B, and -C; see Table S1 in the online Supporting Information). A gravity corer was used to sample the uppermost ~1 m of sediment (short cores). Coring locations (Figure 1b, Table S1) were chosen on the basis of the seismic data to (i) find paleolake sediments beyond the reach of the Eibsee rock avalanche (in the west), (ii) recover Eibsee rock avalanche material with entrained organic matter for radiocarbon dating, and (iii) track multiple stages of catchment response in the aftermath of the catastrophic event, including possible further events, stages of lake rebirth, and basin-wide environmental processes. The long cores EIB16-09A–C, EIB16-09D–F, and EIB16-09G–H at location 4 were recovered with an overlap of ~1.5 m to compile a composite core. This composite core includes a gravity core at the same site to secure the sediment–water interface (Table S1). Coring was stopped when the corer head reached rock material (locations 1, 2, and 4) or a log (location 3).

[Correction added on 05 December 2020, after first online publication: The in-text citations and reference to the companion article "Knapp et al., 2020" were previously missing and have been added in this version]

Lake-sediment analysis

Sediment cores were refrigerated at 4 °C in the lacustrine core-storage facilities at the University of Bern. A GEOTEK Ltd multisensor core logger measured the gamma-ray density, magnetic susceptibility, and *P*-wave velocity with a sampling resolution of 0.5 cm. The PVC tubes were then split lengthwise into two halves, photographed (Geotek Linescan camera), and described by macro- and microscopic analyses of grain size and material. The composite cores were constrained with tie points (marker horizons) where possible (Table S1). The final composite sections at the four locations range in length from 1.05 to 4.71 m. The lowermost sections EIB16-09E, -F, and -H were scanned using computer tomography (CT) at the Institute of Forensic Medicine, University of Bern to highlight differences in density at high resolution and in 3D.

Radiocarbon dating

Accelerator mass spectrometer (AMS) radiocarbon dating was done at the Laboratory for the Analysis of Radiocarbon with AMS (LARA), University of Bern. Radiocarbon ages were reported by the laboratory with 1σ uncertainty. For calibration, we applied OxCal v.4.3.2 (Ramsey, 2017), using the IntCal13 calibration curve from Reimer *et al.* (2013) and the 2σ range.

Geomorphic interpretation

A hillshade 3D digital elevation model (DEM; Bavarian Surveying and Mapping Authority, 2006) of the main depositional area north of Lake Eibsee was used for geomorphic interpretation (see also Part I, Knapp et al., 2020). Field investigation and a geological map (Hornung and Haas, 2017) provided further information. Satellite images were used to detect potential scarps and to assume travel paths of the landslides.

Results and Interpretations

Seismic stratigraphy

The seismic signal penetrated to depths of up to 5 m below the lake floor, except in the easternmost part of the lake where gas masked the stratigraphy. We defined four seismic sequences (seismic units I–IV) on the basis of their geometries and seismic characteristics (Figures 2 and 3).

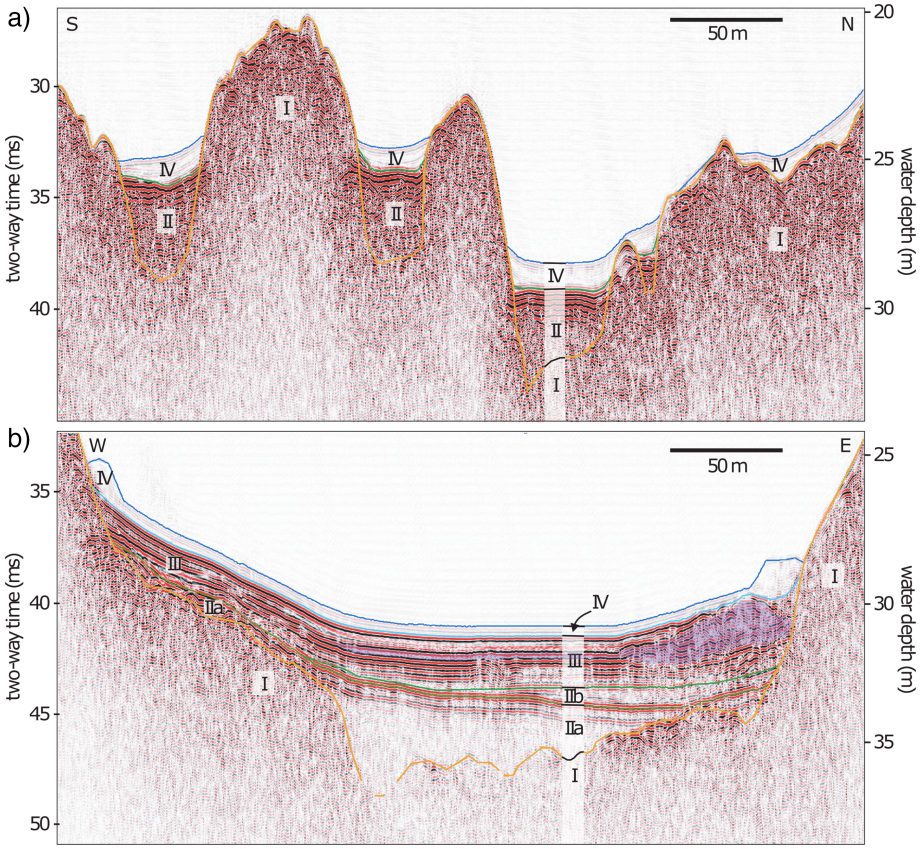

Figure 2. Two seismic profiles from the western (a) and eastern (b) parts of Lake Eibsee (see Figure 1bfor locations). The seismic stratigraphy comprises four seismic sequences labelled I–IV. Seismic unit III occurs only in the eastern, deep basin and contains a mass-movement deposit marked with purple colour. [Colour figure can be viewed at wileyonlinelibrary.com]

Seismic unit I

Seismic unit I is the lowermost sequence. Its upper surface scatters all seismic energy and thus forms the acoustic basement. This surface is highly irregular and bumpy (Figures 2a, b and 3a), and has local relief of 10 m or more.

Seismic unit II (a, b)

Seismic unit II fills the depressions at the top of the unit I topography and generally has a flat upper surface. It is up to 5 m thick and shows at the top parallel high-amplitude reflections resulting from its very strong impedance relative to overlying low-impedance sediments (Figure 2a). In the eastern basin, unit II can be subdivided in lower (IIa) and upper (IIb) subunits (Figure 2b). Subunit IIa occurs in sediment pockets on top of unit I characterized by chaotic or transparent seismic facies and has, when compared to the western basins (Figures 2a and 3a), lower amplitudes on top. It is overlain by a topography-filling, onlapping unit with low-amplitude reflections (subunit IIb) that further flattens out the relief (Figure 2b).

Seismic unit III

Unit III is found only in the eastern, deep basin (Figure 2b). It is up to 3 m thick and is characterized by horizontal medium-to-high-amplitude reflections. A chaotic convex-shaped mound occurs at the toe of the slope at the east side of the deep basin and is interpreted to be a mass-movement deposit originating from the slope to the east (purple colour in Figure 2b).

Seismic unit IV

The uppermost seismic unit is characterized by very low-amplitude reflections, indicating water-rich low-impedance sediments (Figures 2 and 3). It has a maximum thickness of 1.5 m and occurs in the same depressions as units I and II. Unit IV has geometries with slightly curved edges that onlap onto the acoustic basement (unit I). In the deep, eastern basin, these edges have prominent mound structures indicating downslope movement of sediment at the toe of slopes (Figure 2b).

Core lithostratigraphy

About 15 m of lake sediments was retrieved from the four core sites (2.11, 2.17, 1.05, and 4.71 m at locations 1, 2, 3, and 4, respectively; Figures 4 and 5; Table S1). We subdivided the sediment sequences into four lithostratigraphic units.

Lithostratigraphic unit A

Lithology. Unit A is the lowest unit and was retrieved only at location 4, at a composite depth of ~4.5–4.71 m. Its base is marked by large boulders of light-beige Wetterstein Limestone, only a few centimetres of which were penetrated. Core images and CT data indicate that these pieces of limestone are overlain by a layer of cobble-sized clasts with a greyish, silty to sandy matrix (Figure 5).

Correlation and interpretation. Lithostratigraphic unit A correlates with seismic unit I, and hence comprises the acoustic basement (Figure 2b). The rugged surface of seismic unit I, the lack of penetration of the 3.5 kHz signal, and an inability to core unit A with the exception of the single large block at the base of the core at location 4, indicates that this unit is the carapace of a rock avalanche comprising massive boulders underlying the entire modern lake bed. We name this largest and highest-energy event ‘rock-slope failure event 1’.

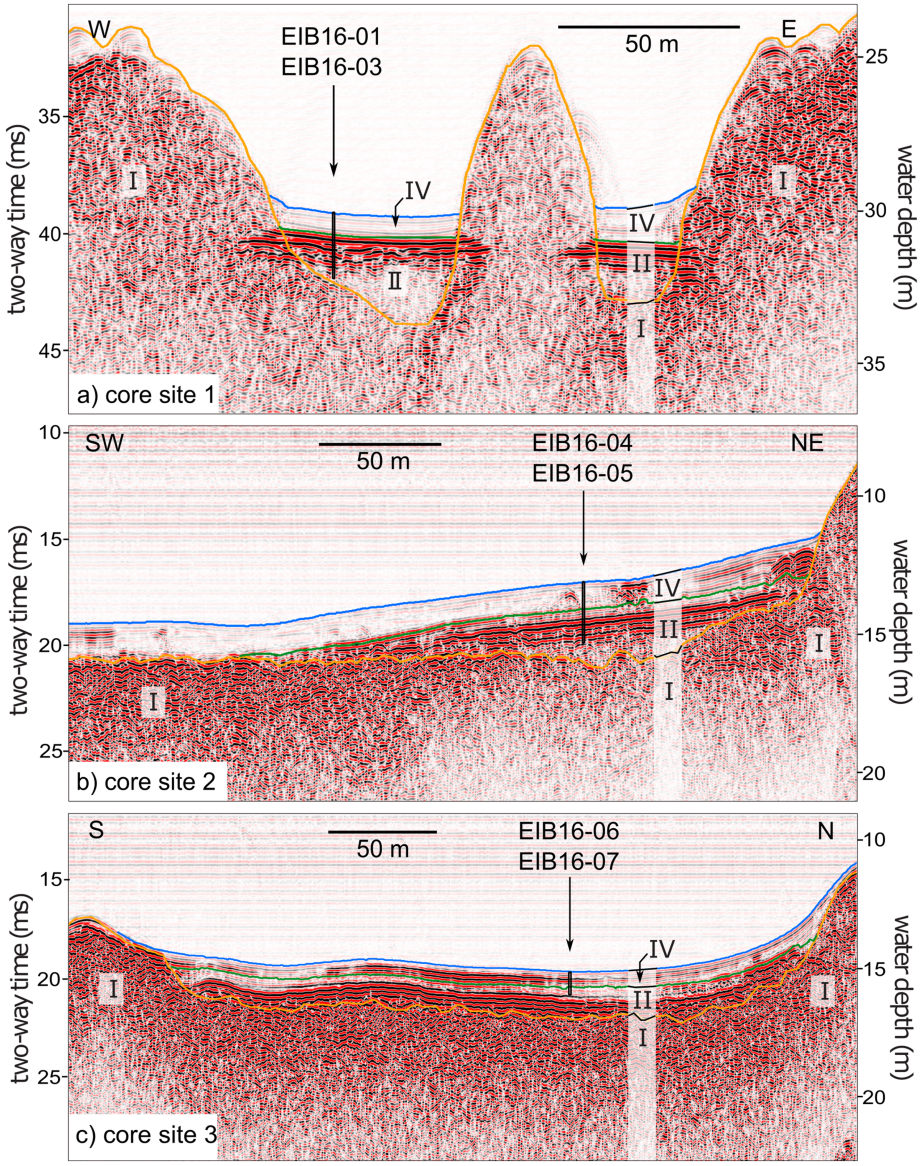

Figure 3. Seismic profiles at core sites 1, 2, and 3 (see Figure 1bfor locations). Seismic units as in Figure 2. [Colour figure can be viewed at wileyonlinelibrary.com]

Lithostratigraphic unit B

Lithology. This unit is present at all four core sites (Figures 4 and 5) at composite depths of ~0.6–2.1 m (site 1), ~1.0–2.2 m (site 2), ~0.9–1.1 m (site 3), and ~1.7–4.5 m (site 4). It comprises angular gravel- to cobble-sized fragments of Wetterstein Limestone and Alpine Muschelkalk embedded in a grey, silty to sandy matrix. Dark grey-brown limestones and marlstones of the Reifling Formation contrast markedly with light grey clasts of Wetterstein Limestone (Figure 5; composite depth ~4.1–4.2 m). Unit B has high-density CT scan values and exhibits normal grading over a vertical distance of many decimetres (~0.8 m at site 1, Figure 4a; ~0.5 m at site 2, Figure 4b; ~1.0 m in the main lake basin at site 4, Figure 5). Two or more graded sections are present, and fragments of wood are common in a cap of fine sediments at the top of the unit.

At site 4, the base of unit B (~4.3–4.5 m composite depth) consists of clay and silt (Figure 5) with low density values. The measured density values and visual observations indicate upward coarsening of this interval, with an increase in amounts of sand, granules, and small pebbles (composite depth ~4.20–4.45 m). The fine-grained upper part of unit B (composite depth ~1.7–2.1 m) is characterized by four normally graded layers with stepwise up-core decrease in layer thickness (18, 12, 8, and 4 cm) and a decrease in basal grain size (Figure 5).

Correlation and interpretation. Unit B coincides with seismic unit II. The overall normal grading indicates deposition during a single event; we term this event 'rock-slope failure event 2'. We interpret the fine layer capping unit B to be a megaturbidite related to a highly-fluidized slurry wave that crossed the rock avalanche material, with fine gravel in suspension.

At site 4, the four graded, subsequent and stacked sediment sections indicated as 'swashes' in Figure 5c are interpreted to be the deposits of a seiche. The seiche is an oscillating wave moving back and forward, which affects the whole lake basin and produces stacked turbidites with up-core fining basal grain sizes, as the basal flow velocity decreases with every passage; they correlate to the seismic subunit IIb. The coarser, graded deposits at the base of litho-unit B here at site 4 coincide with the lower seismic subunit IIa and are interpreted to be debris infilling depressions on the Event 1 deposits. The sharp contact with the underlying lithostratigraphic unit A (seismic unit I) is interpreted as marked by a hiatus, the erosive boundary between rock-slope failure events 1 and 2. The very fine sediment and low density at the very bottom of lithostratigraphic unit B (composite depth ~4.3–4.5 m) indicate dust-cloud

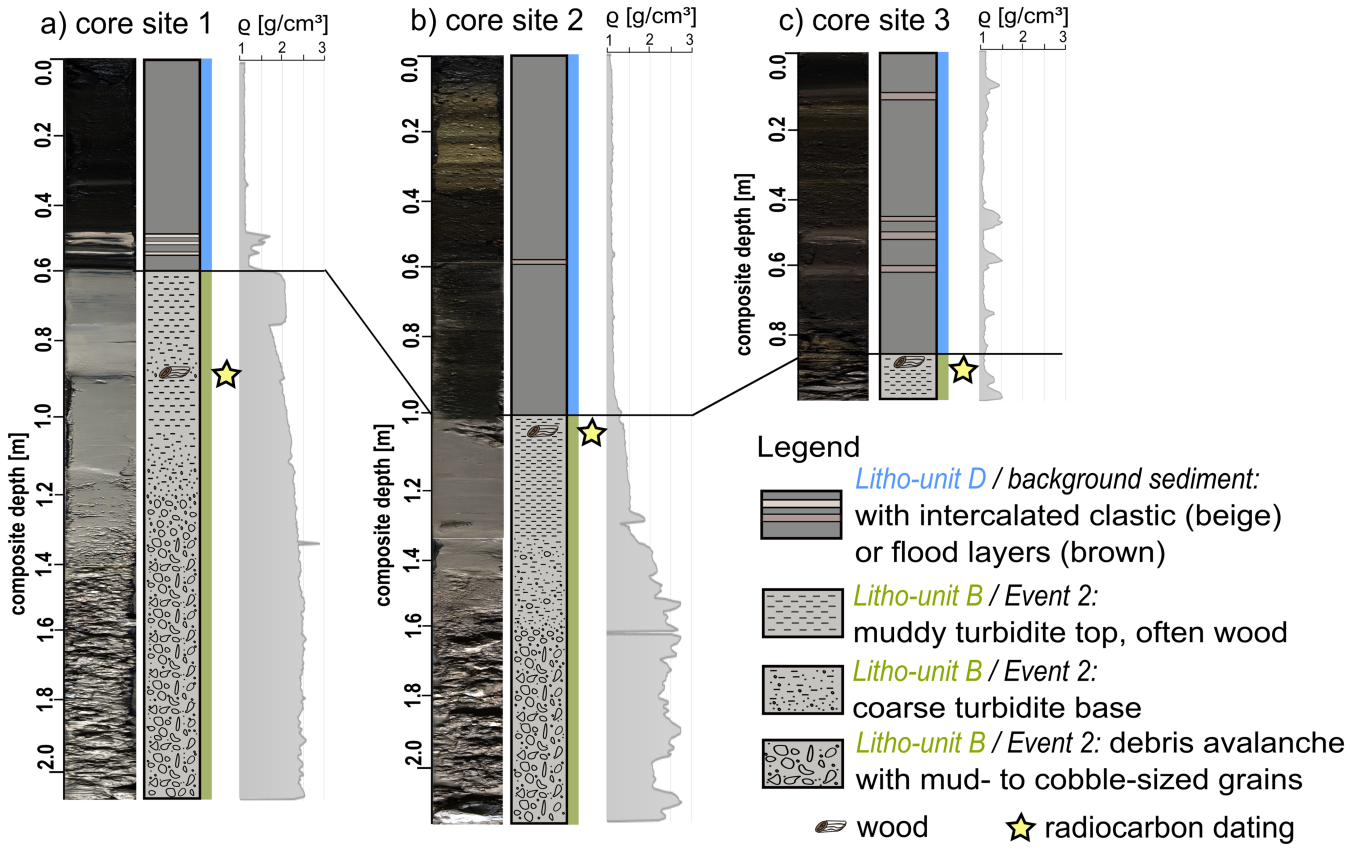

Figure 4. Core-to-core correlation with photographs, sedimentological descriptions, and density profiles at locations 1, 2, and 3 in the western and middle parts of the lake. [Colour figure can be viewed at wileyonlinelibrary.com]

deposits of Event 1, which are partially reworked due to the entrainment during Event 2.

Lithostratigraphic unit C

Lithology. This unit occurs only at site 4 in the deepest basin, at a composite depth of ~0.9–1.7 m (Figure 5). The fine-grained grey sediment has an overall medium density and is generally structureless, with only a few laminations and intercalated coarser layers with wood and leaf fragments, and Fe-oxides.

Correlation and interpretation. Unit C correlates with seismic unit III and is interpreted to be post-event 2 infill. Reworked, shallow-water, marshy sediment was deposited in the flattest and deepest part of the lake basin.

Lithostratigraphic unit D

Lithology. This unit consists of generally dark, jelly-like, low-density sediment rich in organic matter with a few intercalated clastic layers and rare small molluscs.

Its thickness is ~0.6 m at site 1, ~0.8 m at site 3, ~0.9 m at site 4, and ~1.0 m at site 2. At site 4, a normally graded, low-density layer consisting mainly of terrestrial organic matter capped by light-grey silt and clay occurs at ~0.8–0.9 m composite depth.

At sites 1 and 4, several higher-density, centimetre-scale, normally graded, white-beige silt/clay layers occur at composite depths of ~0.5 and ~0.6 m, respectively. Also present in unit B are reddish-brown layers with higher density values that contain abundant terrestrial organic matter (Figure 4; location 2 at ~0.6 m; location 3 at 0.1, ~0.5, and 0.6 m).

Correlation and interpretation. Lithologic unit D correlates with seismic unit IV and records the normal, background organic-rich deposition in the lake (gyttja). The edge-draping geometry reflects redeposition of low-density jelly-like material during storm events. The lower part of the lithologic unit D is dominated by light-coloured clastic layers with down-core increasing density values (Figures 4a and 5a). We interpret these layers to cause the strong acoustic reflection between seismic units III and IV and a slight mismatch between the lithologic C–D and the seismic III–IV boundaries, as the clastic layers belong to unit D, not unit C. We interpret the clastic layer at ~0.8–0.9 m depth to be a turbidite capped by dust-cloud deposits, produced by a third event that we term 'rock-slope failure event 3'. This event was likely of smaller magnitude than events 1 and 2. Other intercalated clastic layers in unit D in the cores at sites 2 and 3 may record rainstorms with heavy runoff that flush into the western part of the lake. Ephemeral streams enter the lake near these two coring sites at the west margin of the lake.

Age of rock-slope failures

Radiocarbon ages of nine wood samples recovered from cores at four coring sites are presented in Table 1. The oldest sample BE-6932.1.1 (10 122 ± 55 yr BP) was collected from the megaturbidite bed (EIB16-03A) at site 1. The calibrated age range is 12 012–11 405 cal yr BP. This sample is much older than was expected; we interpreted it to be reworked and thus removed it from further consideration. Figure 6 summarizes the dating results pertinent to the events we describe in this paper, with coloured rectangles showing overlaps of the 2σ ranges of calibrated ages for the three events.

Event 1 dates to 4089–3876 cal yr BP. With six overlapping sample ages, Event 2 dates to 4082–3976 cal yr BP. The two events cannot be separated based on radiocarbon ages.

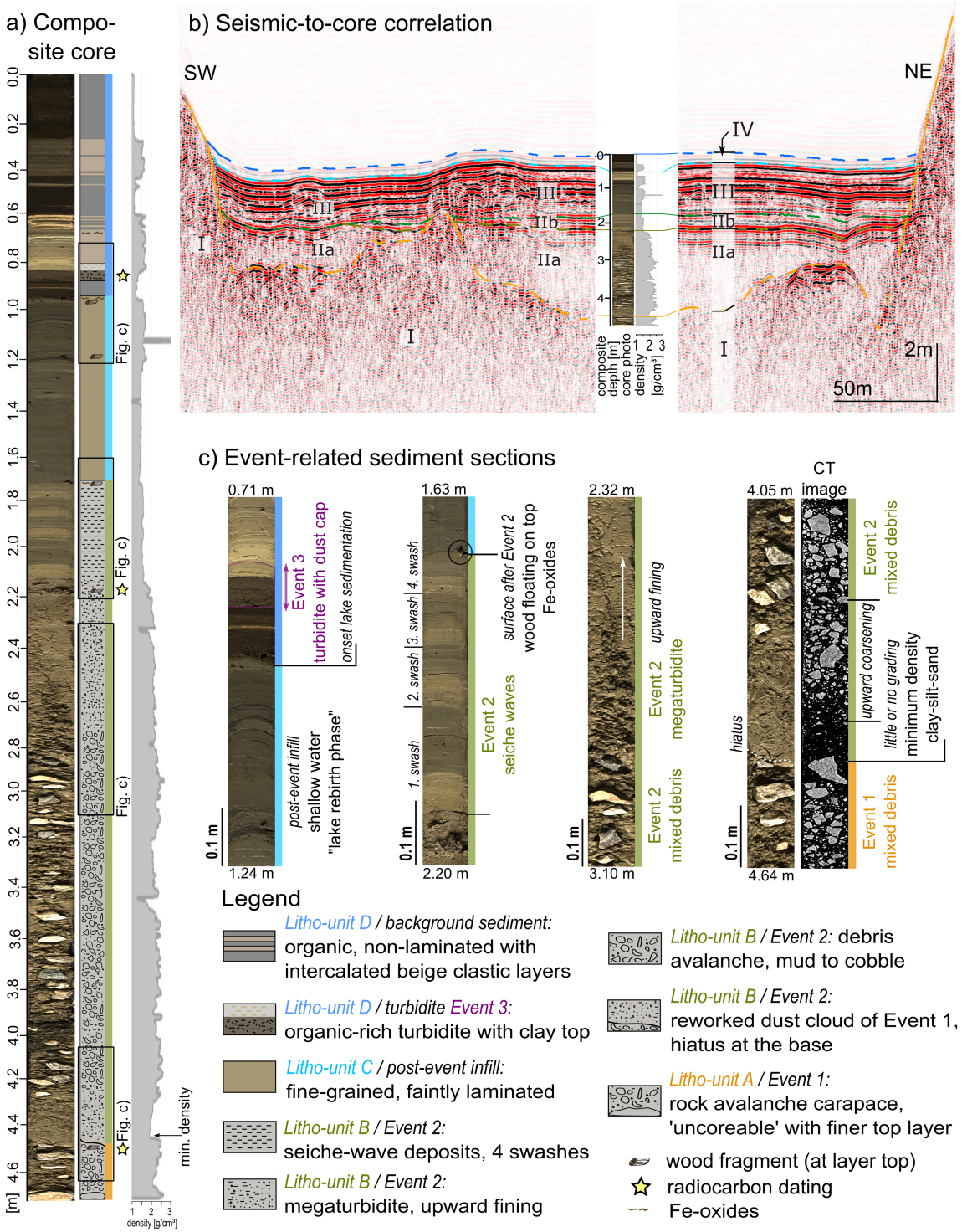

Figure 5. Photographs, sedimentological descriptions, and density profile of composite core from the eastern lake basin. (a) Complete composite core with lithology and density values. (b) Correlation of seismic units and lithologic units. (c) Details of important event-related sediment sections and CT image of the core base. [Colour figure can be viewed at wileyonlinelibrary.com]

However, because Event 1 is older than Event 2, the age of Event 1 can be refined to 4089–3976 cal yr BP. Sample BE-6935.1.1 from the turbidite bed in core EIB16-09A returned a radiocarbon age of 3459 ± 35 cal yr BP and thus provides a calibrated age range of 3830–3640 cal yr BP for Event 3.

Geomorphic interpretation

In addition to the lake deposits, we also examined and mapped sediments and landforms around Lake Eibsee to distinguish different events. Slope analysis reveals flat plains north, west, and southwest of Zirmerskopf (Figure 7a). Sediments beneath these plains infill depressions within the Event 1 deposits. There are two plains, one at ~1000 m a.s.l. north of Zirmerskopf and a second one at ~1030 m a.s.l. west of Zirmerskopf (Figure 7b). The latter slopes stepwise towards the east to ~1026 m a.s.l. and then ~1017 m a.s.l. We interpret these plains to be the result of water runoff towards the northeast during and after Event 2, which infilled the lower basin of the paleolake north of Zirmerskopf (see Figures 3b and c in Part I, Knapp *et al.*, 2020).

A 3D hillshade of the area (Figure 7c) displays our interpretation of how the highly-fluidized mass of Event 2 entered and

Table 1. Radiocarbon ages

Section	Sample lab code	Sediment depth (m)	Material	^{14}C age (BP)	Cal age (BP) (2σ range)	Event
EIB16-09A	BE-6935.1.1	0.35–0.36	wood	3459 ± 35	3830–3640	3
EIB16-09B	BE-6936.1.1	0.80	wood	3630 ± 41	4083–3840	2
EIB16-07	BE-6934.1.1	1.02	wood	3660 ± 19	4082–3907	2
EIB16-07	BE-6934.2.1	1.02	wood	3675 ± 19	4085–3929	2
EIB16-09B	BE-6936.2.1	0.80	wood	3689 ± 47	4151–3896	2
EIB16-05AB	BE-6933.2.1	0.64–0.66	wood	3693 ± 34	4148–3926	2
EIB16-05AB	BE-6933.1.1	0.64–0.66	wood	3725 ± 34	4221–3976	2
EIB16-09H	BE-6937.1.1	0.66	wood	3655 ± 37	4089–3876	1
EIB16-03A	BE-6932.1.1	0.18	wood	10 122 ± 55	12 012–11 405	old

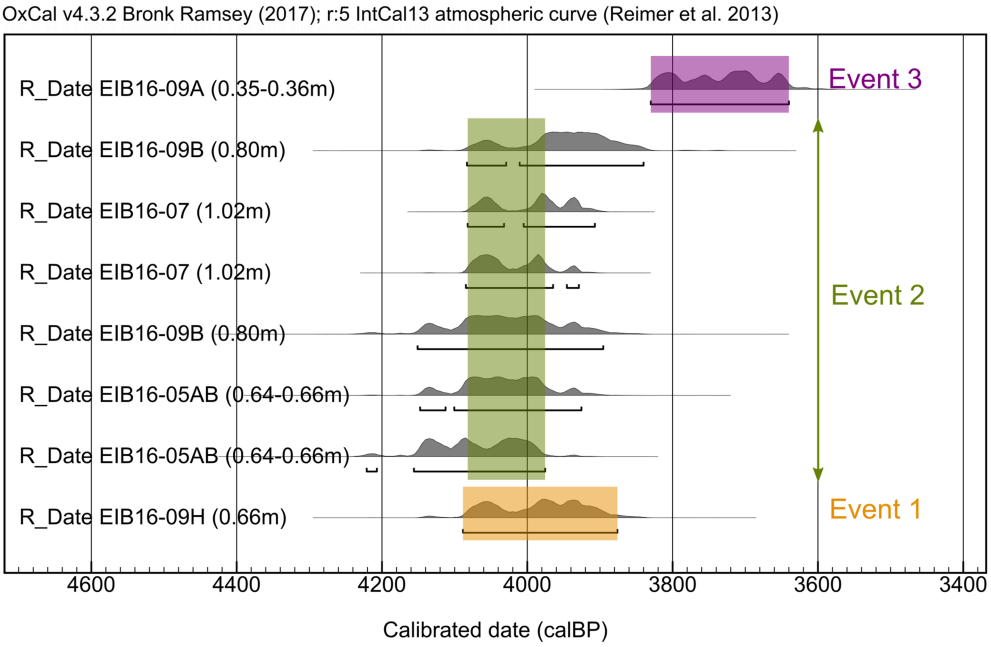

Figure 6. Radiocarbon ages of wood samples recovered from cores, calibrated with OxCal v.4.3.2. Events 1 and 2 are roughly 4000 years old and cannot be separated based on their calibrated age ranges. Event 3 occurred sometime between about 3830–3640 years ago. [Colour figure can be viewed at wileyonlinelibrary.com]

infilled the depressions beyond the Lake Eibsee shoreline. Flowing from the lake, it probably overran the Event 1 deposits at a nickpoint between Plattenkalk bedrock to the west and the Event 1 deposits to the east. Figure 7c also shows Event 3 deposits to the east with levees to both sides.

Discussion

Here we discuss the three stages in Holocene evolution of the landscape at Lake Eibsee, potential triggers of the massive rock-slope failure from Mount Zugspitze, its impact on the paleolake, and the 'lake rebirth' phase.

The rock avalanche, subsequent mass movements, and rebirth of Lake Eibsee

The Eibsee rock avalanche (Event 1) occurred about 4000 years ago when 150-200 million m^3 of limestone fell from the north flank of Mount Zugspitze (Haas *et al.*, 2014; Leith *et al.*, 2016). The seismic reflection survey showed that the rock avalanche deposits are distributed over the entire lake floor. A western lobe of the rock avalanche encountered a rising bedrock slope, and debris became stacked 10–20 m higher there than in other parts of the lake (Figure 1c). An eastern lobe overtopped the paleodam and ran towards Garmisch-Partenkirchen. The main lobe, however, flowed directly to the north through the paleolake (see Part I for details on interactive processes with the substrate). After deposition, the rock avalanche dust cloud presumably covered the whole area, and rainfall washed loose material into small valleys and depressions. Pools grew, merged, and started to build new small lakes with rock avalanche blocks and ridges between them (Figure 8a).

At this stage, a second rock-slope failure occurred (Figure 8b). The rock mass flowed into the shallow lake and entrained the water and dust of the Eibsee rock avalanche. In the distal facies, some centimetres of fine-grained sediment remained between the deposits of the first and second event (Figure 5a, at ~4.1–4.2 m composite depth at core site 4). Therefore, we assume that event 2 did not displace or entrain the underlying loose material, but rather first caused rapid loading (Hungr and Evans, 2004). Due to the loading, the fine sediment was compacted and consolidated, which is indicated by the up-core increase in density despite little or no change in grain size. This process is interpreted to follow the conceptual model developed by Yarnold (1993; Figure 9), who hypothesized on the subaqueous runout of a rock avalanche. His conceptual model describes the interaction of the flowing rock mass with a lake floor and underlying fine-grained sediments. Three stages are differentiated, during which the rock avalanche debris (Figure 9a) entrains sediment, creating a

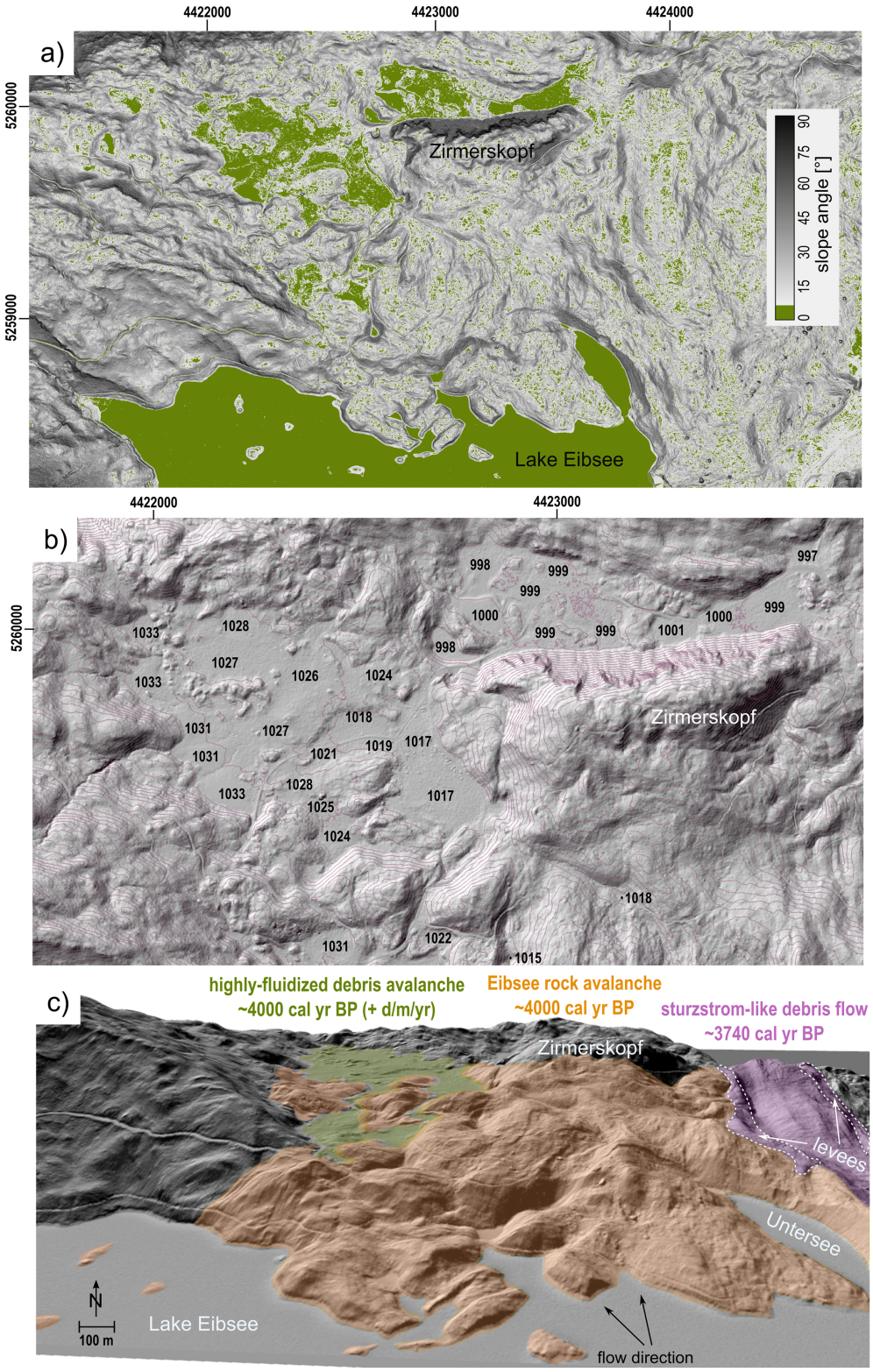

Figure 7. Geomorphology of the area north of Lake Eibsee. (a) Slope angle map showing nearly horizontal plains within the hummocky rock avalanche deposits. (b) Topographic map with 5 m contour lines showing the stepwise southeastward decrease in the elevation of the plain west of Zirmerskopf, and the lower plain north of Zirmerskopf. (c) Geomorphic interpretation in 3D view. All figures are based on a high-resolution 1 m DEM hillshade (Bavarian Surveying and Mapping Authority, 2006). Coordinates are given in Gauss-Krüger Zone 4. [Colour figure can be viewed at wileyonlinelibrary.com]

'contamination zone' at the base of the flow, and becomes more and more plastic (Figure 9b), culminating with slip, but little scour before coming to rest (Figure 9c).

The highly-fluidized debris infilled depressions on the rock avalanche deposits (Figures 2 and 3a, initial filling like in Lake Oeschinen; Knapp *et al.*, 2018), overtopped rock avalanche debris at the north shore, and continued to the north until Zirmerskopf (Figure 7c). After the debris avalanche came to rest, coarse material settled down and finer and lighter material such as wood was deposited on top (Figures 4 and 5). The deposits formed the plains described above (Figures 7a and b). Sediment from the adjacent slopes was washed into the newly formed Lake Eibsee (litho-unit C).

Event 3 generated a large debris flow that travelled straight to the north, with a small western branch reaching the young 'reborn' lake (Figure 8c), thereby generating a turbidite

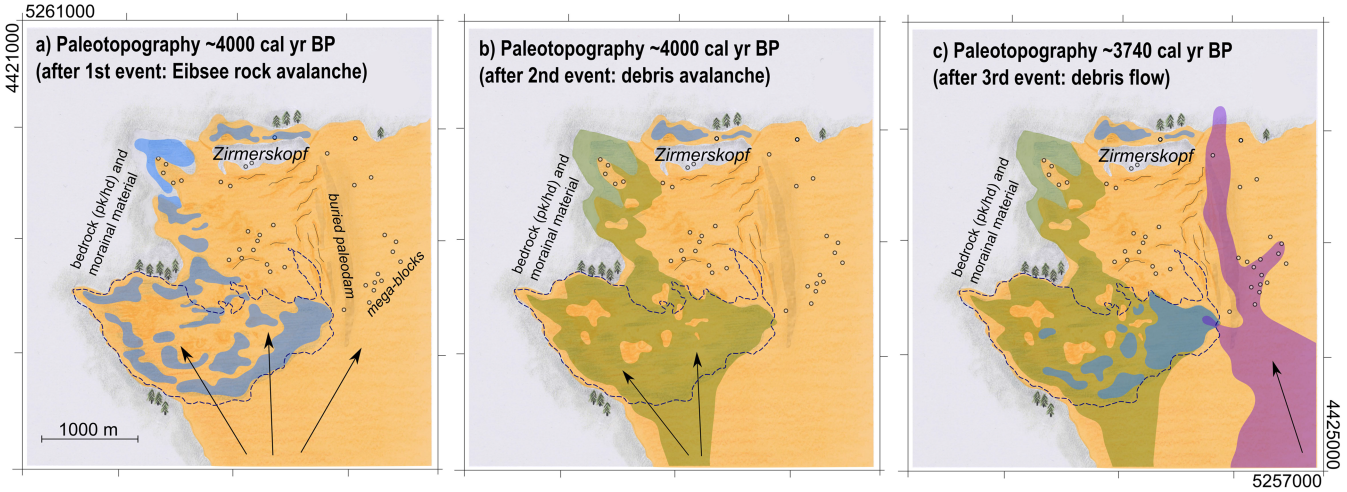

Figure 8. Synoptic sketch of landscape evolution around Lake Eibsee. (a) Eibsee rock avalanche (orange). (b) Debris avalanche (green) ~4000 cal yr BP. (c) Debris flow ~3740 cal yr BP (purple). Dashed line delineates modern Lake Eibsee. hd = Hauptdolomite, pk = Plattenkalk Limestone. Coordinates are given in Gauss-Krüger Zone 4. [Colour figure can be viewed at wileyonlinelibrary.com]

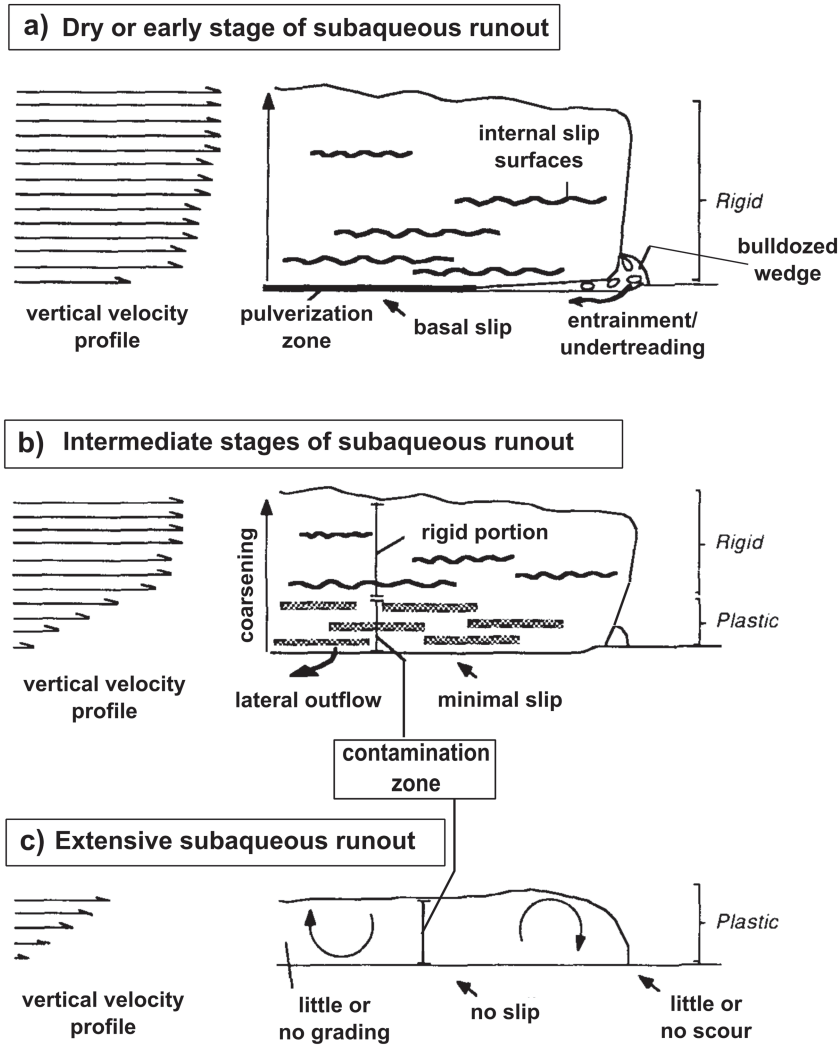

Figure 9. Modified conceptual model of subaqueous runout of a rock avalanche (redrawn from Yarnold, 1993).

(Figures 2 and 5) that interrupted the organic background sediments accumulating in the eastern basin. Fe-oxides and wood and leaf fragments in the sediment cores (Figure 5) indicate that the modern lake was shallow, which might explain the small amount of background sediment produced since Event 3, about 3700 years ago.

Today, Lake Eibsee drains to the north through the permeable rock avalanche deposits. Groundwater is retained by the clayey marlstones of the Allgäu Formation and flows around the Zirmerskopf. Here, the paleolake basin was not filled with rock avalanche deposits, and the ground surface is relatively low (~980 m a.s.l., Figure 7b). Swamps and wetlands in this area

are interpreted to be remnants of Paleolake Eibsee prior to the Eibsee rock avalanche (see Figure 7 in Part I, Knapp *et al.*, 2020).

Classification of rock-slope failures

We recognize and characterize three large rock-slope failures. The classification of the landslides follows Hungr *et al.* (2014). Event 1, the Eibsee rock avalanche, was a massive rock-slope failure in carbonate rocks high on Mount Zugspitze (Abele, 1974; Jerz and Poschinger, 1995). The rock avalanche impacted Paleolake Eibsee and displaced its waters (Part I). The deposits show characteristics of dry rock avalanches with a carapace of mega-blocks (Krieger, 1977; Yarnold and Lombard, 1989; Shaller, 1991; Miller *et al.*, 2017).

Event 2 presumably started as a rock slide or rock avalanche similar to Event 1, but with much smaller volume and lacking mega-blocks. When entering the lake, we hypothesize that the rock mass entrained the available water. Partial or complete saturation of the sediments led to fluidization of the mass (Iverson, 2005; McArdell *et al.*, 2007; Schneider *et al.*, 2011). Without confinement in an established channel but rather widespread shallow deposition, we interpret Event 2 to be a debris avalanche (type 25; Hungr *et al.*, 2014). Similar cases have been reported, for example, by Plafker and Ericksen (1978), Shaller (1991), Hungr and Evans (2004), and Hewitt (2006). The Event 2 rock mass may have detached from the Bayerisches Schneekar on Mount Zugspitze, thereby deepening the scarp niche of Event 1, or from a small scarp directly to the east (Figure 10).

Event 3 is classified as a rock-slope failure, which transformed into a sturzstrom-like debris flow (type 19 or 22; Hungr *et al.*, 2014) that detached from Mount Hohe Riffel (Hornung and Haas, 2017) east of Mount Zugspitze. The debris ran ~4.5 km northward, leaving remarkable levees (Figure 7c). Possible scarp niches and travel paths are shown in Figure 10.

Re-dating of events

Jerz and Poschinger (1995) obtained radiocarbon ages on seven wood samples recovered during drilling at Grainau IV and V (see Figure 1 in Part I for location). The ages range from 3615 ± 65 to 4915 ± 120 yr BP. They assumed that the Eibsee rock avalanche was ~3700 ^{14}C years old.

Our samples from event deposits in Lake Eibsee yielded new chronological information. The Lake Eibsee sediments clearly do not record steady background deposition, as they are dominated by the event deposits: (i) large mass movements ran across the lake, displaced or entrained lake water; (ii) a turbidity current during a less energetic event might be trapped in one basin or trough; and (iii) some of the core sites may have been dry during the rebirth of the lake. Case (ii) happened at ~3740 cal yr BP when a mass movement entered the lake from the southeast; the related turbidite was found only at core site 4 (Figure 5). Thus, to establish an event stratigraphy in Lake Eibsee it is essential to recognize and correctly interpret superimposed event deposits. We compare our new radiocarbon ages with the previous ages from the Grainau drill cores, which we re-calibrated with OxCal v4.3.2 (see Figure S1 in the online Supporting Information).

Disregarding the outlier of samples BE-6932.1.1, which is probably reworked, and BE-6935.1.1, which marks the debris flow event at ~3740 cal yr BP, all other lake samples yielded ages ~4000 cal yr BP and date the Eibsee rock avalanche and the debris avalanche in its aftermath (events 1 and 2). All our ages overlap at 2σ to a period of 113 years, but it is not possible to further refine the ages of events 1 and 2. The sediment between these two events, however, suggests an interval of at least some days or weeks to allow settling of dust and fine-grained sediment on top of the Eibsee rock avalanche mass, and enough time to fill a shallow lake, but probably not more than a few years or decades because there is no evidence of soil development.

Predisposing factors and potential triggers

The Eibsee rock avalanche happened at the end of the second Holocene climate optimum (Wanner *et al.*, 2008). Climate cooled and became wetter ~4000–3700 cal yr BP

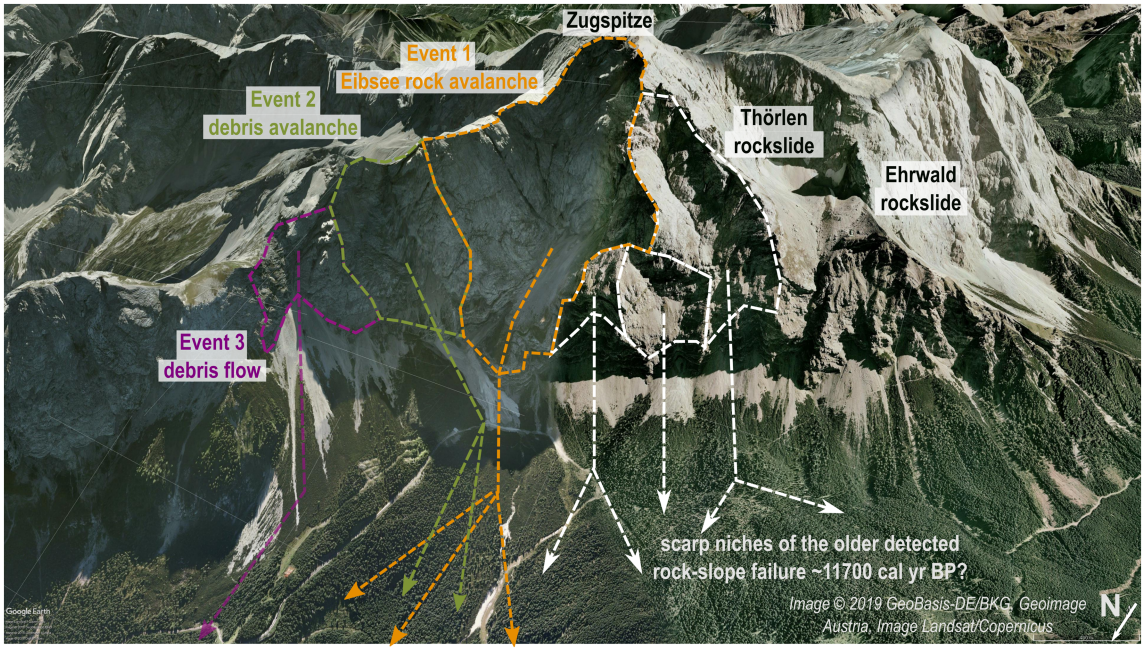

Figure 10. Potential scarps and travel paths of the mass movements documented in this paper. The scarp of Event 2 is oriented to the northwest. The neighbouring scarps may be related to older rock-slope failures (white polygons and arrows, see Table 1). Satellite image © 2019 GeoBasis-DE/BKG, Geoimage Austria, Image Landsat/Copernicus. [Colour figure can be viewed at wileyonlinelibrary.com]

(Heiri *et al.*, 2003), possibly gradually destabilizing the steep limestone rock slopes at Mount Zugspitze. Karst weathering favours the formation of cavities around the summits of the massive carbonate platform rocks in the Wetterstein Mountains (Hornung and Haas, 2017). In the case of events 2 and 3, the loss of rock mass in the headwall of the Bayerisches Schneekar during the Event 1 rock avalanche may have weakened the surrounding rock masses.

A possible earthquake trigger must also be considered, given that Mount Zugspitze is located in a seismically active region near the Loisach-Fernpass fault and the Inn Valley fault (Figure 1a; Linzer *et al.*, 2002; Lenhardt *et al.*, 2007; Nasir *et al.*, 2013). Our new dating results and recalibration of the previously published ages enable a better evaluation of possible coincidences in the Fernpass rockslide cluster. The Fernpass rockslide has been dated at ~4150 ± 100 cal yr BP using the U/Th method (Ostermann *et al.*, 2007). Other events in the Fernpass cluster include the Pletzachkogel landslide dated at ~3910 cal yr BP (Prager *et al.*, 2008; Patzelt, 2012b), the Stöttlbach landslide dated at 3800 ± 660 cal yr BP (Prager *et al.*, 2008), and megaturbidites generated by subaqueous landslides in Lake Piburg and Lake Plansee at ~4000 cal yr BP (Oswald *et al.*, 2020). The new results of the limnogeological studies at Lake Eibsee, Lake Piburg, and Lake Plansee, which are within a radius of 30 km, increase the likelihood that a large prehistoric earthquake triggered the Eibsee rock avalanche.

Conclusions

We identify and date three rock-slope failures at Lake Eibsee using a combination of lake core sedimentology and radiocarbon dating, geophysical surveys in the lake, and geomorphological analysis: (i) the Eibsee rock avalanche at ~4000 cal yr BP; (ii) a debris avalanche in the aftermath of the rock avalanche, presumably from the same scarp or a neighbour; and (iii) a sturzstrom-like debris flow from Riffelriss at ~3740 cal yr BP.

We radiocarbon-dated the Eibsee rock avalanche at four sites in modern Lake Eibsee to 4089–3976 cal yr BP, which is about the same age as major rockslides in the Fernpass cluster. The possible coincidence in ages makes a large earthquake a possible trigger.

Age dating alone does not conclusively disclose the failure history. A multimethodological approach is important to refine recurrence rates. In contrast to the Tschirgant rock avalanche, where dating results first indicated two events (Patzelt, 2012a), but which Ostermann *et al.* (2017) later concluded was a single event, the Eibsee rock avalanche deposits suggest two events, the ages of which cannot be discriminated by radiocarbon dating.

The multiple events in the Lake Eibsee record provide evidence for successive failures of the Mount Zugspitze scarp niche.

There are three Eibsee lakes: (i) the original and largest one existed until the Eibsee rock avalanche (Event 1), about 4000 years ago (Paleolake 1; see Part I); (ii) several shallow ponds separated by islands that formed in the aftermath of the massive rock avalanche and lasted until the debris avalanche of Event 2 (Paleolake 2); and (iii) the modern Lake Eibsee, which started to form soon after Event 2.

Paleolake sediments were not retrieved at any of the coring sites because the piston corer could not penetrate the carapace of Event 1. However, geophysical data indicate that the entire lake floor is underlain by Event 1 deposits.

Acknowledgements—Sibylle Knapp acknowledges PhD funding from the German National Academic Foundation (Studienstiftung des deutschen Volkes e.V.). Radiocarbon dating was financially supported by the British Society for Geomorphology through a postgraduate research grant to Sibylle Knapp. We thank the Rieppel family for allowing us to do fieldwork on Lake Eibsee. Verena Stammberger, Christoph Mayr, Ioannis Kouvatsis, and the Wasserwacht Garmisch-Partenkirchen supported fieldwork. Andreas von Poschinger provided drill-hole logs, and Ulrich Haas contributed to discussions during this study. Open access funding enabled and organized by Projekt DEAL.

Conflict of Interest

The authors declare that they have no conflict of interest.

Data Availability Statement

The datasets used and/or analysed during the current study are available from the corresponding author on reasonable request.

References

Abele G. 1974. Bergstürze in den Alpen. Ihre Verbreitung, Morphologie und Folgeerscheinungen. *Wissenschaftliche Alpenvereinshefte* **25**: 1–230.

Bavarian Surveying and Mapping Authority. 2006. *Airborne laser scan (Garmisch)*. München: Bavarian Surveying and Mapping Authority.

Eberhardt E, Stead D, Coggan J. 2004. Numerical analysis of initiation and progressive failure in natural rock slopes—the 1991 Randa rockslide. *International Journal of Rock Mechanics and Mining Sciences* **41**(1): 69–87.

Fan X, Zhan W, Dong X, van Westen C, Xu Q, Dai L, Yang Q, Huang R, Havenith H-B. 2018. Analyzing successive landslide dam formation by different triggering mechanisms: the case of the Tangjiawan landslide, Sichuan, China. *Engineering Geology* **243**: 128–144.

Haas U, Ostermann M, Sanders D, Hornung T. 2014. Quaternary sediments in the Werdenfels region (Bavaria, southern Germany). In *From the Foreland to the Central Alps – Excursion Guide to the Field Trips of the DEUQUA Congress in Innsbruck, Austria, 24–29 September 2014*, Kerschner H, Krainer K, Spötl C (eds). Geozon: Berlin; 18–30.

Heiri O, Lotter AF, Hausmann S, Kienast F. 2003. A chironomid-based Holocene summer air temperature reconstruction from the Swiss Alps. *The Holocene* **13**(4): 477–484.

Hermanns R, Blikra L, Naumann M, Nilsen B, Panthi K, Stromeyer D, Longva O. 2006. Examples of multiple rock-slope collapses from Köfels (Ötz valley, Austria) and western Norway. *Engineering Geology* **83**(1–3): 94–108.

Hewitt K. 2006. Rock avalanches with complex run out and emplacement, Karakoram Himalaya, Inner Asia. In *Landslides from massive rock slope failure*. Springer; 521–550.

Hornung T, Haas U. 2017. *Erläuterungen zur Geologischen Karte 1:25 000, 8531/8631 Zugspitze 8532/8632 Garmisch-Partenkirchen*. Bavarian Environmental Agency: Augsburg.

Hungr O, Evans S. 2004. Entrainment of debris in rock avalanches: an analysis of a long run-out mechanism. *Geological Society of America Bulletin* **116**(9–10): 1240–1252.

Hungr O, Leroueil S, Picarelli L. 2014. The Varnes classification of landslide types, an update. *Landslides* **11**(2): 167–194.

Iverson RM. 2005. Regulation of landslide motion by dilatancy and pore pressure feedback. *Journal of Geophysical Research – Earth Surface* **110**(F2): 1–16. https://doi.org/10.1029/2004JF000268

Ivy-Ochs S, Heuberger H, Kubik P, Kerschner H, Bonani G, Frank M, Schlüchter C. 1998. The age of the Köfels event – relative, ^{14}C and cosmogenic isotope dating of an early Holocene landslide in the Central Alps (Tyrol, Austria). *Zeitschrift für Gletscherkunde und Glazialgeologie* **34**: 57–68.

Jerz H, Poschinger A. 1995. Neuere Ergebnisse zum Bergsturz Eibsee-Grainau. *Geologica Bavarica* **99**: 383–398.

Knapp S, Gilli A, Anselmetti FS, Krautblatter M, Hajdas I. 2018. Multi-stage rock-slope failures revealed in lake sediments in a seismically active alpine region (Lake Oeschinen, Switzerland). *Journal of Geophysical Research – Earth Surface* **123**(4): 658–677.

Knapp S, Mamot P, Lempe B, Krautblatter M. 2020. Impact of an 0.2 km^3 Rock Avalanche on Lake Eibsee (Bavarian Alps, Germany) – Part I: Reconstruction of the paleolake and Effects of the Impact. *Earth Surf. Process. Landforms*. https://doi.org/10.1002/esp.5024

Krieger MLH. 1977. *Large landslides, composed of megabreccia, interbedded in Miocene basin deposits, southeastern Arizona*, Vol. **1008**. U.S. Government Printing Office: Washington, D.C.

Leith K, Hofmayer F, Kessler B, Krautblatter M. 2016. *Preconditioning of the Eibsee rock avalanche by deglaciation and development of critical bedrock stresses*, paper presented at the EGU General Assembly Conference.

Lenhardt WA, Freudenthaler C, Lippitsch R, Fiegweil E. 2007. Focal-depth distributions in the Austrian Eastern Alps based on macroseismic data. *Austrian Journal of Earth Sciences* **100**: 66–79.

Linzer H-G, Decker K, Peresson H, Dell'Mour R, Frisch W. 2002. Balancing lateral orogenic float of the Eastern Alps. *Tectonophysics* **354**(3–4): 211–237.

McArdell BW, Bartelt P, Kowalski J. 2007. Field observations of basal forces and fluid pore pressure in a debris flow. *Geophysical Research Letters* **34**(7): 1–4. https://doi.org/10.1029/2006GL029183

Miller GS, Andy Take W, Mulligan RP, McDougall S. 2017. Tsunamis generated by long and thin granular landslides in a large flume. *Journal of Geophysical Research, Oceans* **122**(1): 653–668.

Nasir A, Lenhardt W, Hintersberger E, Decker K. 2013. Assessing the completeness of historical and instrumental earthquake data in Austria and the surrounding areas. *Austrian Journal of Earth Sciences* **106**(1): 90–102.

Ostermann M, Sanders D, Prager C, Kramers J. 2007. Aragonite and calcite cementation in "boulder-controlled" meteoric environments on the Fern Pass rockslide (Austria): implications for radiometric age dating of catastrophic mass movements. *Facies* **53**(2): 189–208.

Ostermann M, Ivy-Ochs S, Sanders D, Prager C. 2017. Multi-method (^{14}C, ^{36}Cl, $^{234}U/^{230}Th$) age bracketing of the Tschirgant rock avalanche (Eastern Alps): implications for absolute dating of catastrophic mass-wasting. *Earth Surface Processes and Landforms* **42**(7): 1110–1118.

Oswald P, Huang J-JS, Fabbri S, Aufleger M, Daxer C, Strasser M, Moernaut J. 2020. *Strong earthquakes as main trigger mechanism for large pre-historic rock slope failures in Western Tyrol (Austria, Eastern Alps): constraints from lacustrine paleoseismology*, paper presented at the EGU General Assembly Conference Abstracts, Vienna.

Patzelt G. 2012a. Die Bergstürze von Tschirgant und von Haiming, Oberinntal, Tirol–Begleitworte zur Kartenbeilage. *Jahrbuch der Geologischen Bundesanstalt* **152**(1–4): 13–24.

Patzelt G. 2012b. Die Bergstürze vom Pletzachkogel, Kramsach, Tirol. *Jahrbuch der Geologischen Bundesanstalt* **152**(1–4): 25–38.

Plafker G, Ericksen G. 1978. Nevados Huascaran avalanches, Peru. In *Developments in Geotechnical Engineering*, Vol. **14**. Elsevier; 277–314.

Prager C, Zangerl C, Patzelt G, Brandner R. 2008. Age distribution of fossil landslides in the Tyrol (Austria) and its surrounding areas. *Natural Hazards and Earth System Sciences* **8**: 377–407.

Prager C, Ivy-Ochs S, Ostermann M, Synal H-A, Patzelt G. 2009. Geology and radiometric ^{14}C-, ^{36}Cl- and Th-/U-dating of the Fernpass rockslide (Tyrol, Austria). *Geomorphology* **103**(1): 93–103.

Ramsey CB. 2017. Methods for summarizing radiocarbon datasets. *Radiocarbon* **59**(6): 1809–1833.

Reimer PJ, Bard E, Bayliss A, Beck JW, Blackwell PG, Ramsey CB, Buck CE, Cheng H, Edwards RL, Friedrich M, Grootes PM. 2013. IntCal13 and Marine13 radiocarbon age calibration curves 0–50,000 years cal BP. *Radiocarbon* **55**(4): 1869–1887.

Schneider D, Huggel C, Haeberli W, Kaitna R. 2011. Unraveling driving factors for large rock–ice avalanche mobility. *Earth Surface Processes and Landforms* **36**(14): 1948–1966.

Shaller PJ. 1991. Analysis of a large moist landslide, Lost River range, Idaho, USA. *Canadian Geotechnical Journal* **28**(4): 584–600.

Walter F, Amann F, Kos A, Kenner R, Phillips M, de Preux A, Huss M, Tognacca C, Clinton J, Diehl T, Bonanomi Y. 2020. Direct observations of a three million cubic meter rock-slope collapse with almost immediate initiation of ensuing debris flows. *Geomorphology* **351**: 106933.

Wanner H, Beer J, Bütikofer J, Crowley TJ, Cubasch U, Flückiger J, Goosse H, Grosjean M, Joos F, Kaplan JO, Küttel M. 2008. Mid- to Late Holocene climate change: an overview. *Quaternary Science Reviews* **27**(19–20): 1791–1828.

Wanner H, Solomina O, Grosjean M, Ritz SP, Jetel M. 2011. Structure and origin of Holocene cold events. *Quaternary Science Reviews* **30**(21–22): 3109–3123.

Yarnold JC. 1993. Rock-avalanche characteristics in dry climates and the effect of flow into lakes: insights from mid-Tertiary sedimentary breccias near Artillery Peak, Arizona. *Geological Society of America Bulletin* **105**(3): 345–360.

Yarnold JC, Lombard JP. 1989. A facies model for large rock-avalanche deposits formed in dry climates.

Supporting Information

Additional supporting information may be found online in the Supporting Information section at the end of the article.

Table S1: Sediment-core locations, types and correlation. EIB16-02, EIB16-09D and EIB16-09G were not used for correlation. Coordinates are given in Gauss-Krüger Zone 4.

Figure S1: Comparison of calibrated, previously published radiocarbon ages on the Eibsee rock avalanche and our ages from Lake Eibsee. Our ages overlap at 4089–3976 cal yr BP.

